

Intercalating TOP2 poisons attenuate topoisomerase action at higher concentrations

Mandeep Atwal, Rebecca L. Swan, Chloe Rowe, Ka C. Lee, David C Lee, Lyle Armstrong, Ian G Cowell*, Caroline A Austin*

Running title: Inhibition by doxorubicin, epirubicin and mitoxantrone

MA, RLS, CR, KCL, IGC, CAA Institute for Cell and Molecular Biosciences, Newcastle University, Newcastle upon Tyne. NE2 4HH. U.K.

DCL, LA Institute of Genetic Medicine, Newcastle University, International Centre for Life, Central Parkway, Newcastle upon Tyne. NE1 3BZ.

DCL: <https://orcid.org/0000-0001-6857-624X>

IGC: <https://orcid.org/0000-0002-8606-0447>

CAA: <https://orcid.org/0000-0002-1921-5947>

*Corresponding authors:

Ian G Cowell & Caroline A Austin

Institute for Cell and Molecular Biosciences, Newcastle University, Newcastle upon Tyne NE2 4HH. United Kingdom

Tel: +44 (0)191 208 7677

Fax: +44 (0)191 208 7424

Email: ian.cowell@ncl.ac.uk, caroline.austin@ncl.ac.uk

30 text pages (including refs and figure legends)

8 figures

0 tables

60 number of references

219 words in abstract

641 words in Introduction

1268 words in Discussion

Abbreviations

DMSO	Dimethyl sulfoxide
DOX	Doxorubicin
DSB	Double-strand break
EPI	Epirubicin
ICRF-193	4-[2-(3,5-Dioxo-1-piperazinyl)-1-methylpropyl]piperazine-2,6-dione
TARDIS	Trapped in Agarose DNA Immunostaining assay
TOP2	Topoisomerase II
TOP2A	Topoisomerase II α
TOP2B	Topoisomerase II β
TOP2-CC	Topoisomerase II covalent complex

Abstract

TOP2 poisons are effective cytotoxic anticancer agents that stabilise the normally transient TOP2-DNA covalent complexes formed during the enzyme reaction cycle. These drugs include etoposide, mitoxantrone and the anthracyclines, doxorubicin and epirubicin. Anthracyclines also exert cell-killing activity via TOP2-independent mechanisms including DNA adduct formation, redox activity and lipid peroxidation. Here we show that anthracyclines and another intercalating TOP2 poison mitoxantrone stabilise TOP2-DNA covalent complexes less efficiently than etoposide and at higher concentrations they suppress the formation of TOP2-DNA covalent complexes, thus behaving as TOP2 poisons at low concentration and inhibitors at high concentration. We employed iPSC-derived human cardiomyocytes as a model to study anthracycline induced damage in cardiac cells. We demonstrated for the first-time using immunofluorescence the presence of TOP2B as the only TOP2 isoform in iPSC derived cardiomyocytes. In these cells etoposide robustly induced TOP2B-covalent complexes, but we could not detect doxorubicin-induced TOP2-DNA complexes, and doxorubicin suppressed etoposide-induced TOP2-DNA complexes. *In vitro*, etoposide-stabilised DNA cleavage was attenuated by doxorubicin, epirubicin or mitoxantrone. Clinical use of anthracyclines is associated with cardiotoxicity. The observations in this study have potentially important clinical consequences regarding the effectiveness of anticancer treatment regimens when TOP2 targeting drugs are used in combination. These observations suggest that inhibition of TOP2B activity rather than DNA damage resulting from TOP2 poisoning may play a role in doxorubicin cardiotoxicity.

Significance statement

We show that anthracyclines and mitoxantrone act as TOP2 poisons at low concentration but attenuate TOP2 activity at higher concentration, both in cells and in *in vitro* cleavage experiments. Inhibition of type II topoisomerases suppresses the action of other drugs that poison TOP2. Thus, combinations containing anthracyclines or mitoxantrone and etoposide, may reduce the activity of etoposide as a TOP2 poison and thus reduce the efficacy of drug combinations.

Introduction

Human type II DNA topoisomerases (TOP2) are highly effective anti-cancer drug targets, but TOP2 targeting drugs (TOP2 poisons) can cause short and long-term side effects including neutropenia, therapy related leukaemia and cardiotoxicity (Cowell and Austin, 2012; De Angelis *et al.*, 2016). Anthracyclines target TOP2 and also act via additional mechanisms including lipid peroxidation, redox activity and drug-DNA crosslink formation (Winterbourn *et al.*, 1985; Bodley *et al.*, 1989; Sinha *et al.*, 1989; Capranico, Kohn, *et al.*, 1990; Gewirtz, 1999; Swift *et al.*, 2006; Coldwell *et al.*, 2008). However, they can induce serious complications in cardiac and myeloid cells even at doses under the maximum recommended lifetime exposure limit. Tailored tests are reducing the number of patients receiving cytotoxic chemotherapy (Sparano *et al.*, 2018), but anthracycline-containing chemotherapy regimens are still recommended for many patients including children and adolescents. Thus, it is important to understand the mechanism by which the adverse effects arise to be able to modify current treatment regimens to reduce side effects. Recently, TOP2B was implicated in cardiotoxicity, as murine cardiomyocytes lacking TOP2B are protected from doxorubicin damage (Zhang *et al.*, 2012).

Drugs that target TOP2 fall into at least two categories; TOP2 poisons such as etoposide (Long *et al.*, 1984) and catalytic inhibitors such as ICRF-187 (Roca *et al.*, 1994; Classen *et al.*, 2003). TOP2 poisons stabilize the TOP2-DNA covalent complex when DNA is in the cleaved position leading to the accumulation of TOP2-DNA complexes within the cell that can result in cell death (Cowell and Austin, 2012). TOP2 catalytic inhibitors antagonise the action of TOP2 poisons and therefore may be used in combination with TOP2 poisons to reduce the side effects arising from TOP2 poison therapy (Reichardt *et al.*, 2018).

Early *in vitro* studies and *in cellulo* studies of anthracycline interactions with TOP2 found a bell shaped concentration-dependence in the induction of DNA cleavage (Capranico, Kohn,

et al., 1990; Capranico, Zunino, *et al.*, 1990; Ferrazzi *et al.*, 1991; Willmore *et al.*, 2002). *In vitro* cleavage on pBR322 DNA showed doxorubicin cleavage at low concentrations, but less at higher concentrations (Tewey *et al.*, 1984). The same effect was observed using *in vitro* end-labelled PMC41 DNA in cleavage assays (Bodley *et al.*, 1989), or *in vitro* end labelled SV40 DNA (Binaschi *et al.*, 1998). In addition to suppression of *in vitro* cleavage, higher concentrations of doxorubicin and epirubicin attenuated teniposide and amsacrine (Capranico, Kohn, *et al.*, 1990; Capranico, Zunino, *et al.*, 1990). These early *in vitro* cleavage experiments used topoisomerase II enzyme purified from murine L1210 cells, which contained a mixture of the two isoforms TOP2A and TOP2B. Using SDS/KCl to precipitate protein-DNA complexes doxorubicin stabilised fewer protein-DNA complexes compared to an equitoxic dose of etoposide in the rat glioblastoma cell line C6 (Montaudon *et al.*, 1997), no accumulation of TOP2-DNA complexes was observed in KB cells following doxorubicin treatment (Suzuki *et al.*, 1997). Using immunological assays specific for TOP2-DNA complexes such as the trapped in agarose DNA immunostaining assay (TARDIS) and the in-vivo-complex-of-enzyme (ICE) assay, which produce robust signals when cells are treated with etoposide, TOP2-DNA complexes were detectable under some conditions with mitoxantrone, idarubicin, epirubicin and doxorubicin (Willmore *et al.*, 2002; Errington *et al.*, 2004; Smart *et al.*, 2008; Hasinoff *et al.*, 2016; Atwal *et al.*, 2017). In this study we confirm using the TARDIS assay that mitoxantrone, doxorubicin and epirubicin stabilise covalent TOP2-DNA complexes at lower concentrations, demonstrating poisoning activity; but that fewer complexes are stabilised at higher concentrations in cells, indicating inhibition of activity. Inhibition by mitoxantrone, doxorubicin and epirubicin was compared to the catalytic inhibitor ICRF-193. *In vitro* experiments using recombinant TOP2A or TOP2B demonstrated that decatenation by either isoform was inhibited by mitoxantrone, doxorubicin or epirubicin and that etoposide-induced cleavage by either isoform was attenuated by mitoxantrone, doxorubicin or epirubicin. Biphasic poisoning/inhibition of TOP2 has potential implications for the pharmacokinetics of anthracyclines in cancer therapy.

Materials and Methods

Reagents and antibodies

Doxorubicin, epirubicin, etoposide and mitoxantrone, dimethyl sulfoxide, Tween 20, Triton X-100 and paraformaldehyde were purchased from Sigma-Aldrich (Dorset, UK). ICRF-193 was purchased from Biomol, Germany. kDNA was purchased from Inspiralis (Norwich, UK). Plasmid TCS1 was a gift from T.Hsieh (Lee *et al.*, 1989) and supercoiled plasmid DNA was purified using caesium chloride centrifugation. Recombinant human TOP2A and human TOP2B were produced as described in (Wasserman *et al.*, 1993; West *et al.*, 2000). Anti-TOP2 polyclonal antibodies raised in rabbits were used to conduct experiments. 4882 anti-TOP2 was raised to topoisomerase II purified from calf thymus, this protein was a ~140KDa N-terminal fragment lacking the C-terminal region based on partial peptide sequencing, and was a mixture of TOP2A and TOP2B (Austin *et al.*, 1990). Antibodies 4566 and 4555 were raised to the C-terminal domain of recombinant human TOP2A (residues 1244-1531) or recombinant human TOP2B (residues 1263-1621) respectively. These antibodies were developed in-house (see supplemental data Fig.1). Anti-mouse γ H2Ax (Cat# 05-636) was obtained from Merck-Millipore, UK.

Decatenation assays

200ng kDNA was incubated in reaction buffer (50 mM Tris.HCl (pH7.5), 125 mM NaCl, 10 mM MgCl₂, 5 mM DTT and 100 μ g/ml albumin), with or without drug, as indicated in the figure legends, the reaction volume was 20 μ l, reactions were initiated by the addition of TOP2A or TOP2B and incubated for 30 minutes at 37°C. Loading buffer was added and samples were run on a 0.8% gel in TBE (100mM Tris-borate pH8.3, 2mM EDTA). Gels were stained with ethidium bromide after electrophoresis and visualised on a BioRad EZ gel doc.

DNA cleavage assays

pTCS1 DNA substrate (3.9µg) was incubated in reaction buffer (10mM Tris-HCl pH8.0, 10mM MgCl₂, 50mM KCl, 150µg/ml BSA and 1mM ATP) in the presence or absence of mitoxantrone, doxorubicin or epirubicin with or without etoposide for 30 minutes at 37°C. The reactions were initiated by the addition of 1.2µg TOP2A or TOP2B, the reaction volume was 100µl. Reactions were terminated by addition of SDS to 1%, followed by addition of EDTA to 25mM and proteinase K to 0.5mg/ml and incubated for 60 minutes at 45°C. The DNA was precipitated overnight at -20°C following the addition of sodium acetate to 300mM and the addition of 2 volumes of ethanol. The DNA precipitate was collected by centrifugation and the pellet air dried prior to resuspension in 15µl TE, 5µl of loading buffer was added and the samples were heated to 70°C for 2 minutes prior to running on a 0.8% agarose gel in TAE buffer (40mM Tris, 2mM EDTA & 0.11% (v/v) glacial acetic acid), in the presence of ethidium bromide. Gels were visualised on a BioRad EZ gel doc and bands were quantified by ImageLab v.5.2.1 (BioRad).

Cell culture

NB4 and K562 cells were maintained in RPMI-1640 medium supplemented with 10% fetal bovine serum and 1% penicillin and streptomycin (Thermo Fischer Scientific, Paisley, UK). Cells were cultured at 37°C in a humidified atmosphere containing 5% CO₂. Experiments were conducted on exponentially growing cells (2-5 x 10⁵ cells/mL). NB4 (DSMZ ACC-207) and K562 (ATCC CCL-243) cell lines (Lozzio and Lozzio, 1975; Lanotte *et al.*, 1991) were originally sourced from the DSMZ and ATCC respectively. Cells were routinely tested for mycoplasma infection.

Undifferentiated induced pluripotent stem cells (iPSCs) were maintained in feeder free culture with GFR Matrigel (Corning) and mTeSR1 (StemCell Technologies, Cambridge U.K.) with 1% Pen/Strep, these cells were tested monthly for mycoplasma and were originally sourced from Lonza. Differentiation to induced pluripotent stem cell derived cardiomyocytes was performed using an established protocol followed by metabolic purification (Lian *et al.*,

2013) (Tohyama *et al.*, 2013). Briefly, iPSCs were cultured as described above to form a confluent monolayer; at this point (day 1 of the protocol) the medium was changed to a base differentiation medium consisting of RPMI 1640 supplemented with B27 minus insulin and 1% Pen/Strep (Life Technologies, UK) and 9µM CHIR99021 trihydrochloride (Tocris, Abingdon U.K.). On day 2 the medium was changed to base medium. On day 4 the medium was changed to a mixture of fresh basal medium and the existing medium from the culture in a 1:1 ratio; this was supplemented with 5µM IWP2 (Tocris). The medium was changed to base medium on day 6 and on day 8 the medium was changed to maintenance medium consisting of RPMI 1640 supplemented with 2% B27 and 1% Pen/Strep. On day 10 the medium was changed to metabolic purification medium consisting of RPMI-1640 without glucose, supplemented with 2% B27 and 1% Pen/Strep. On day 15 the medium was replaced with maintenance medium. Thereafter the maintenance medium was changed every 2-3 days. Cardiomyocytes generated using this protocol were characterised by FACS analysis of SIRPA expression (Dubois *et al.*, 2011) followed by Q-PCR quantification of sarcomeric marker genes (ACTN2, TNNT2, TNNI3, MYH6 and MYH7) and detection of their respective proteins by immunohistochemistry (data not shown). Cardiomyocyte function was assessed by observation of spontaneous contraction and recording spontaneous calcium transients.

Trapped in Agarose DNA Immunostaining (TARDIS) assay.

The TARDIS assay was used to quantify the level of stabilised TOP2-DNA covalent complexes *in situ*, conducted as previously described (Willmore *et al.*, 1998; Cowell *et al.*, 2011). Briefly, cells were treated for 1 hour with the desired TOP2 poison. Cells were pelleted (1000xg, 5mins) and washed in ice-cold PBS. After re-centrifugation cells were mixed in an equal volume of molten 2% LMP agarose (Lonza, Basel, Switzerland) in PBS and spread evenly onto agarose-coated slides. Agarose-embedded cells were lysed (1% w/v SDS, 20mM sodium phosphate, 10mM EDTA, pH 6.5) and non-covalently bound DNA proteins were removed using 1M NaCl. Stabilised TOP2 covalent complexes were detected

by immunofluorescence using anti-TOP2 rabbit polyclonal antibodies followed by Alexa-488 coupled anti-rabbit secondary antibodies (Thermo Fischer Scientific). Slides were counterstained with Hoechst 33258 (Thermo Fischer Scientific) to visualise DNA. Images were captured for Hoechst and Alexa-488, using an epifluorescence microscope (Olympus IX-81, 10x objective) fitted with an Orca-AG camera (Hamamatsu) and suitable narrowband filter sets. Image capture and automated slide scoring was performed using Volocity 6.3 software (PerkinElmer Inc.). Briefly, acquired images were each processed to identify nuclei by thresholding the DAPI signal. After filtering to separate or remove touching/overlapping objects (nuclei) the immunofluorescent signal emanating from each nucleus was determined to produce a table of integrated fluorescence per nucleus. Parameters to select individual nuclei were set up at the beginning of the analysis for one slide, and these parameters were then used for all other slides in the experiment. Data are represented using GraphPad Prism 8.0 or 8.1 and R (San Diego, CA).

Immunofluorescence Analysis of γ H2AX

After drug treatment, cells were washed and pelleted in ice-cold PBS and spotted on poly-L-lysine coated slides. Cells were fixed in 4% paraformaldehyde in PBS for 10 minutes and permeabilised using KCM+T buffer (120mM KCl, 20mM NaCl, 10mM Tris-HCl pH 8.0, 1mM EDTA, 0.1% Triton-X-100) for 15 minutes. After blocking (KCM+T, 2% bovine serum albumin, 10% dry milk powder) cells were probed with anti- γ H2Ax in blocking buffer followed by Alexa-594 anti-mouse secondary antibodies. Slides were counterstained with DAPI. Images were captured for DAPI and Alexa-594 and quantification was performed using Volocity 6.3 (PerkinElmer Inc.) as described for the TARDIS assay.

Statistics

Statistical analysis was performed using Graph Pad Prism 8.0. The details of the tests performed are given in figure legends. For signifying *P* values, * refers to $P < 0.05$, ** refers to $P < 0.01$, *** refers to $P < 0.001$ and **** refers to $P < 0.0001$. Error bars in bar charts represent SD values. The study was designed to be exploratory rather than testing a specific null hypothesis and *p* value are therefore descriptive only. Where intergroup comparisons are made, these were specified in advance of data acquisition. Sample sizes (numbers of replicate experiments) were specified in advance of data acquisition based on prior knowledge of the characteristics of the assays involved and anticipating occasional lost or failed samples.

Results

Etoposide and mitoxantrone both induce stable TOP2-DNA complexes, but with differing concentration responses. TOP2-DNA covalent complexes stabilized by TOP2 poisons such as etoposide can be efficiently and specifically detected using the TARDIS assay (Willmore *et al.*, 1998; Cowell *et al.*, 2011). In this assay cells treated with TOP2 poison are suspended in low-melting point agarose, spread on glass microscope slides and lysed in buffer containing 1% SDS and then extracted in high salt buffer. This treatment removes most cellular constituents, leaving “nuclear ghosts” trapped in the agarose which consist of nuclear DNA and any covalently attached proteins. TOP2A or TOP2B-covalent DNA complexes can then be detected and quantified on a single cell basis by immunofluorescence. In this way, the median fluorescent signal per nucleus and the distribution of nuclear signal intensities can be determined. For the archetypal epipodophyllotoxin TOP2 poison etoposide, TOP2A complexes can be reproducibly detected with as little as 1 μ M etoposide and TOP2B complex induction can be detected from 10 μ M in mouse and human cells (Willmore *et al.*, 1998; Cowell *et al.*, 2011; Atwal *et al.*, 2017) (Fig. 1A). TOP2 complex levels increased with increasing etoposide concentration up to at least 100 μ M etoposide. TOP2 complexes are processed in the cell to give rise to DNA DSBs that elicit a DNA damage response, including the phosphorylation of histone H2AX. Etoposide-induced levels of H2AX phosphorylation followed a similar dose response as that observed for TOP2-DNA complexes (Fig. 1B).

Mitoxantrone is an anthracenedione TOP2 poison, which unlike etoposide intercalates into DNA with a high affinity (Lown *et al.*, 1984). We have previously shown that mitoxantrone also efficiently induces both TOP2A- and TOP2B-DNA complexes in murine cells, but the quantity of complexes plateaus at approximately 1 μ M mitoxantrone (Errington *et al.*, 1999). We confirm this result here using human NB4 cells (Fig.1C) and demonstrate that at a higher concentration (20 μ M) TOP2A and TOP2B complex levels are reduced, suggesting that mitoxantrone inhibits TOP2-DNA complex formation at elevated concentrations. This

reduction in TOP2-DNA complexes at higher concentrations of mitoxantrone was mirrored in the level of H2AX phosphorylation. Levels of γ H2AX signal peaked with 1 μ M mitoxantrone and decreased at 10 μ M and 20 μ M mitoxantrone (Fig. 1D).

Anthracyclines targeting TOP2 are inefficient at inducing stable TOP2-DNA complexes. Like etoposide and mitoxantrone, anthracyclines including doxorubicin (dox) and epirubicin (epi) are TOP2 poisons on the basis of their ability to increase the steady-state concentration of the covalent TOP2-DNA complexes by impeding religation of DNA (Pommier *et al.*, 2010; Vos *et al.*, 2011). Each of these drugs stimulates cleavage of DNA substrates by TOP2 in *in vitro* assays (Bodley *et al.*, 1989; Capranico *et al.*, 1993; Binaschi *et al.*, 1998). However, unlike etoposide and mitoxantrone, the anthracyclines have not been reported to induce the formation of large numbers of stable TOP2-DNA complexes in cells that can be detected using the TARDIS assay, or the ICE assay (Montaudon *et al.*, 1997; Willmore *et al.*, 2002; Swift *et al.*, 2006; Nitiss *et al.*, 2012). For example, while the anthracycline idarubicin induced a small dose dependent increase in TOP2A complexes up to 1 μ M and a marginal increase in TOP2B complexes over control cells, at 20 μ M fewer TOP2-DNA complexes were seen (Willmore *et al.*, 2002). Doxorubicin-induced TOP2-DNA complexes were not detected in this previous TARDIS study (Willmore *et al.*, 2002).

In this study we were able to detect doxorubicin and epirubicin-induced TOP2A complexes in human NB4 cells using the TARDIS assay (Fig. 2A). This discrepancy may be due to the improved sensitivity of the assay in the current study resulting from the use of brighter, more stable fluorochromes and more sensitive camera technology. However, median fluorescence levels per nucleus did not exceed 20% of the level recorded for the positive control treatment (100 μ M etoposide) and no significant dox or epi signal was observed for TOP2B (Fig. 2A). For both dox and epi only a small increase in median fluorescent signal was observed for TOP2A between 1.0 μ M and 10 μ M. Subsequent experiments were carried out at 10 μ M for both drugs. In line with the reduced level of stabilized TOP2 complexes compared to 100 μ M etoposide, dox and epi both resulted in lower γ H2AX induction than etoposide (Fig. 2B). This

is similar to a previous finding (Huelsenbeck *et al.*, 2012) in rat glioblastoma cells where doxorubicin-induced H2AX phosphorylation was maximal at 2 μ M, and was reduced compared to the extent of phosphorylation induced by 100 μ M etoposide. Since TARDIS analysis provides fluorescence intensity data from individual nuclei, the resulting data can also be presented as the percentage of cells with a signal above a given threshold (Huelsenbeck *et al.*, 2012). We chose 25% of the value of the median signal obtained for 100 μ M etoposide as a convenient threshold. For TOP2A (4566), approximately 5% and 10% of 10 μ M dox and epi-treated cells exceeded this cutoff (Fig. 2C).

The data obtained for Figs 1&2 involved treating cells for 60 minutes with TOP2 poison before carrying out the TARDIS assay. To determine whether the relatively low level of stable TOP2-DNA complexes observed with epi was due to slow complex formation compared to etoposide, a TOP2A TARDIS time-course experiment was performed. Median fluorescence levels induced by epi did not increase with drug incubation times from 30 to 120 minutes (Fig. 3A). The TARDIS assay data shown in Figs 1, 2 and 3A employed antibodies raised to the divergent C-terminal regions of the TOP2A and TOP2B proteins which allows the two isoforms to be analyzed independently (4566 and 4555 respectively, see Supplemental Fig. 1). We were concerned that the low signal observed with the anthracyclines compared to etoposide could be due to epitope masking by post-translational modification or rapid proteolytic removal of the C-terminal domain following anthracycline drug treatment. To test this possibility, we repeated the TARDIS assay with antibody 4882 which was raised to the conserved N-terminal 140kDa of calf thymus TOP2 and detects both isoforms of human TOP2 (see Supplemental Figure 1). Using this antibody, 10 μ M and 100 μ M etoposide produced a robust signal in the TARDIS assay. However, no significant increase in median fluorescence was observed for 10 μ M dox or epi compared to the no-drug control (Fig. 3B&C), while an intermediate level of signal was observed for 20 μ M mitoxantrone. Considering the results obtained with antibodies 4566 (TOP2A CTD), 4555 (TOP2B CTD) and 4882 (TOP2A and B N-terminal 140kDa), the low anthracycline-induced

TOP2A signal and lack of TOP2B signal in the TARDIS assay is not likely to be due to loss or masking of the C terminal domain, indicating inefficient trapping of stable TOP2 complexes by dox and epi.

Doxorubicin, epirubicin and mitoxantrone can inhibit stable TOP2-DNA complexes in competition assays. Various lines of evidence including *in vitro* DNA cleavage data, H2AX phosphorylation and TARDIS data (Bodley *et al.*, 1989; Willmore *et al.*, 2002; Smart *et al.*, 2008; Huelsenbeck *et al.*, 2012) support the idea that intercalating anthracycline TOP2 poisons and mitoxantrone inhibit TOP2 activity at higher concentrations. Competition between poisoning and inhibition may then explain the relatively inefficient generation of stable TOP2-DNA complexes by anthracyclines. To further study this, etoposide-induced TOP2 complexes were quantified using the TARDIS assay in NB4 cells that had been pre-incubated with either 10 μ M dox, 10 μ M epi, 20 μ M mitoxantrone or the well characterized bisdioxopiperazine TOP2 catalytic inhibitor, ICRF-193 (100 μ M)(Patel *et al.*, 2000). As noted previously, the anthracyclines on their own induced a low TOP2A signal compared to that obtained with etoposide, while 20 μ M mitoxantrone alone induced a small but significant TOP2A signal. ICRF-193 did not induce TOP2A or TOP2B complexes significantly above basal levels. However, pre-incubation with each of these drugs significantly inhibited both TOP2A and TOP2B covalent complex formation by etoposide (Fig. 4A&B). Indeed, the level of inhibition achieved by the anthracyclines and mitoxantrone was similar to that observed for ICRF-193. Since NB4 cells contain a high level of MPO activity which increases TOP2 complex formation via oxidative activation of etoposide, we repeated the experiments shown in Fig. 4A&B using the MPO non-expressing cell line K562 (Fig. 4C&D). Very similar results were observed in K562 cells; the anthracyclines efficiently inhibited etoposide-induced TOP2A and TOP2B complex formation at 10 μ M and 100 μ M etoposide. Mitoxantrone also significantly inhibited etoposide induced TOP2B complex formation and TOP2A complexes at 100 μ M etoposide.

Since TOP2 complexes are processed in cells to DSBs that elicit γ H2AX formation, we also determined the ability of dox, epi and mitoxantrone to inhibit etoposide-induced H2AX phosphorylation. As observed in Fig. 2B, the anthracyclines alone at 10 μ M lead to H2AX phosphorylation (Fig. 5), however no signal above background was observed for 100 μ M ICRF-193. Levels of histone H2AX phosphorylation induced by 10 μ M etoposide were not significantly increased or decreased by pre-treatment with dox or epi compared to etoposide alone. While dox and epi alone produce a H2AX signal, no additive effect on DSB formation was observed when the anthracyclines were co-incubated with 10 μ M etoposide. In addition, H2AX phosphorylation induced by 10 μ M etoposide was not reduced by anthracycline treatment. However, pre-incubation with epi, but not dox, did significantly reduce the level of H2AX phosphorylation by approximately 25% following treatment with 100 μ M etoposide. In contrast, etoposide induced H2AX phosphorylation was strongly suppressed by mitoxantrone at both concentrations of etoposide. Indeed, this suppression was greater than that observed for ICRF-193 with 100 μ M etoposide, although the efficacy of inhibition by ICRF-193 may be limited by its solubility in aqueous solution.

Doxorubicin failed to induce detectable TOP2B-DNA complexes in cardiomyocytes derived from iPSCs but did suppress etoposide induced complex formation. Although anthracyclines are widely used and effective anti-cancer drugs, their side-effect profile includes potentially serious cardiac damage (van Dalen *et al.*, 2005). Using iPSC derived cardiomyocytes, we examined the expression of TOP2B and TOP2A by immunofluorescence. As anticipated for fully differentiated cells, only about 5% of the cardiomyocytes expressed significant levels of TOP2A, but all cells expressed abundant TOP2B (Fig 6A). While 100 μ M etoposide efficiently induced TOP2B-DNA complexes in the cardiomyocyte cells, doxorubicin did not induce TOP2B complexes significantly above background levels (Fig. 6B). Moreover, preincubation with 10 μ M doxorubicin suppressed etoposide induced TOP2B complexes in cardiomyocyte cells, confirming that doxorubicin

attenuates TOP2 activity in cardiomyocytes. Thus, the inhibition observed by doxorubicin treatment is not limited to a single cell type.

In vitro inhibition of TOP2 decatenation activity by mitoxantrone, doxorubicin, epirubicin or ICRF-193

In vitro, TOP2 decatenation activity can be analysed using highly catenated kinetoplast DNA (kDNA). As shown in Fig. 7, high molecular weight kDNA remains in the well of an agarose gel (first lane of each panel) and in the absence of drugs TOP2A and TOP2B catalyse the decatenation of kDNA, resulting in the migration into the gel of decatenated circles (second lane of each panel). However, addition of mitoxantrone, dox or epi resulted in a decline in the TOP2-mediated decatenation activity with increasing concentrations of drugs (Fig. 7 A-C). The effect of the catalytic inhibitor ICRF193 is shown for comparison.

In vitro attenuation of etoposide induced DNA cleavage by mitoxantrone, doxorubicin or epirubicin

Data generated using two leukaemia cell lines (NB4 and K562) and iPSC derived cardiomyocytes strongly suggest that mitoxantrone, dox and epi attenuate TOP2 activity thereby blocking the formation of the TOP2-DNA covalent complex which prevents the action of the TOP2 poison, etoposide (Figs 4-6). To further clarify this we conducted *in vitro* DNA cleavage assays to analyse the effects of etoposide induced TOP2 mediated DNA cleavage in the presence of either mitoxantrone, dox or epi. Cleavage experiments were performed using supercoiled plasmid DNA substrate TCS1 in the presence of etoposide and with varying concentrations of mitoxantrone, dox or epi. Increasing concentrations of mitoxantrone, doxorubicin or epirubicin attenuated etoposide-induced plasmid cleavage in a concentration dependent manner (Fig. 8). Etoposide-induced DNA cleavage of both isoforms was reduced by 50% or greater at concentrations of between 4 and 6 μ M mitoxantrone, doxorubicin or epirubicin.

Discussion

This study aimed to evaluate the possible consequences of combining several TOP2 targeting drugs, some of them used in combination in current treatment protocols, in cancer cells with differing characteristics and in iPSC-derived human cardiomyocytes. We used the TARDIS assay to investigate the poisoning of TOP2-DNA complexes by the clinically relevant anthracyclines, doxorubicin and epirubicin, as well as the anthracenedione mitoxantrone. Stabilised TOP2-DNA complexes were detected, albeit at low levels, following treatment of NB4 cells with doxorubicin or epirubicin, consistent with earlier studies.

Unlike etoposide which stabilised TOP2-DNA complexes in a concentration dependent manner in NB4 cells, mitoxantrone produced a bell-shaped curve whereby levels of TOP2A and TOP2B-DNA complexes increase up to 10 μ M but were lower at 20 μ M. This suggests that mitoxantrone acts as a TOP2 poison at lower concentrations and has inhibitory activity at higher concentrations, as previously shown for idarubicin (Willmore *et al.*, 2002). Willmore and colleagues also demonstrated inhibition by idarubicin using the TARDIS competition assay. Specifically, pre-incubation of cells with higher concentrations of idarubicin inhibited the etoposide-induced stabilisation of TOP2-DNA complexes. In the current study, we also used the TARDIS competition assay to evaluate the activity of doxorubicin, epirubicin and mitoxantrone as inhibitors for both isoforms of TOP2. TOP2 catalytic inhibitors reduce the level of etoposide-stabilised complexes, as they result in fewer 'active' TOP2 molecules to bind and cleave DNA. Indeed, pre-incubation with ICRF-193, a well-established catalytic inhibitor of TOP2, substantially reduced the level of etoposide-induced TOP2 poisoning. Pre-incubation with doxorubicin, epirubicin or mitoxantrone also significantly reduced levels of etoposide-induced TOP2A- and TOP2B- DNA complexes (Figure 4A-D). This supports the notion that anthracyclines and mitoxantrone can attenuate TOP2 activity, as suggested previously by *in vitro* cleavage studies (Capranico, Kohn, *et al.*, 1990; Capranico, Zunino, *et al.*, 1990). As doxorubicin, epirubicin and mitoxantrone are DNA intercalators, the inhibition observed at higher concentrations may be due to DNA intercalation reducing access to DNA

rather than direct enzyme inhibition as observed with ICRF-193. Consistent with this, Bodley et al demonstrated that inhibition of TOP2-mediated DNA cleavage by a series of doxorubicin and daunorubicin congeners correlated with their intercalating capacity (Bodley et al., 1989). In the present study (Figure 7) we have shown that mitoxantrone, doxorubicin or epirubicin each inhibit TOP2A or TOP2B mediated decatenation of kinetoplast DNA, an assay used to show inhibition of TOP2. Inhibition of TOP2B-catalysed decatenation by doxorubicin was previously reported (Frank et al., 2016) and inhibition of TOP2A and TOP2B catalysed decatenation was shown for doxorubicin, pixantrone and etoposide by Hasinoff et al, 2016. We also show that *in vitro* cleavage of supercoiled plasmid DNA by etoposide is attenuated by mitoxantrone, doxorubicin or epirubicin in a dose dependent manner (Fig. 8); these *in vitro* experiments show effects at concentrations comparable to the cell-based assays and in patients. Notably, patient-derived C_{max} concentrations for mitoxantrone, doxorubicin and epirubicin measured (0.7 μ M, 7 μ M and 17 μ M respectively) (Liston and Davis, 2017), are comparable to the concentrations that attenuate etoposide cleavage (shown in Fig. 8).

The inhibition of TOP2 by doxorubicin, epirubicin and mitoxantrone were also investigated using the γ H2AX assay to measure levels of drug-induced double strand DNA breaks. While etoposide induced the phosphorylation of histone H2AX in a concentration-dependent manner, γ H2AX levels decrease with increasing concentrations of mitoxantrone above 1 μ M. This is consistent with TARDIS data showing the decrease in TOP2-DNA complex levels at higher concentrations of mitoxantrone. Consistently, levels of etoposide-induced histone H2AX phosphorylation are significantly reduced when cells are pre-incubated with 20 μ M mitoxantrone. In contrast, levels of doxorubicin-induced DSBs increased in a concentration-dependent manner. Furthermore, pre-incubation with doxorubicin did not affect the levels of etoposide-induced DSBs, despite significantly reducing levels of etoposide-induced TOP2-DNA complexes as measured by TARDIS assay. This supports the idea that doxorubicin-induced DNA damage occurs via additional mechanisms beyond TOP2 poisoning which

could include DNA-adduct and free-radical formation (Gewirtz, 1999; Swift *et al.*, 2006; Coldwell *et al.*, 2008). This contrasts with mitoxantrone and ICRF-193, which significantly reduce the etoposide-induced γ H2AX signal (Fig. 5), consistent with their action predominantly through TOP2.

Anthracyclines are used in many successful treatment protocols. However, patients treated with anthracyclines such as doxorubicin and epirubicin can develop serious cardiac complications, even at doses under the maximum recommended exposure limit. The mechanisms of cardiac toxicity are elusive, and many theories have been suggested because anthracyclines appear to act on more than one target. Whereas etoposide performs its cytotoxic action by mainly targeting TOP2 (Chen *et al.*, 1984; Minocha and Long, 1984), it is believed that the anthracyclines (doxorubicin, epirubicin) and mitoxantrone utilize other mechanisms in addition to TOP2 poisoning for cytotoxicity (Tuteja *et al.*, 1997; Gewirtz, 1999; Minotti *et al.*, 2004; Evison *et al.*, 2015). For example, doxorubicin treatment causes marked damage to mitochondria, yet mitochondrial targeting of doxorubicin eliminated the cardiac toxicity (Jean *et al.*, 2015). Studies in murine cardiomyocytes and human pluripotent stem cell derived cardiomyocytes have strongly implicated TOP2B in doxorubicin-induced cardiotoxicity (Zhang *et al.*, 2012; Maillet *et al.*, 2016). Lyu *et al.* proposed a model for the role of TOP2B in cardiotoxicity (Lyu *et al.*, 2007) where anthracycline-induced TOP2B DNA-covalent complexes are processed via proteasomal activity to exposed DNA-DSBs in cardiomyocytes. However, this study did not directly demonstrate the presence anthracycline-induced TOP2-DNA complexes, and as we demonstrate here in lymphoblastoid cells, TOP2B-DNA complexes are induced very inefficiently in cells by anthracyclines. This suggests that the role of TOP2B in anthracycline-induced cardiotoxicity may be less straightforward. Elucidating the mechanism by which TOP2B expression leads to doxorubicin-induced cardiotoxicity may inform cardio-protection strategies in the clinic. To further examine the possible effects of anthracyclines in the light of their complicated mechanisms of TOP2 inhibition, we used iPSC-derived cardiomyocytes. Although these cells

might show differences from the adult cardiomyocyte phenotype, mainly in terms of their metabolism, we show that most iPSC-derived cardiomyocytes do not express TOP2A, whilst TOP2B was expressed in all cardiomyocytes, which should also be true for adult terminally differentiated cardiomyocytes. In our experiments, doxorubicin (1 μ M or 10 μ M) did not induce TOP2B-DNA complexes above the background level in cardiomyocytes, even though complexes were efficiently induced by etoposide (Fig. 6). Furthermore, as was observed in NB4 and K562 cells, doxorubicin inhibited etoposide-induced TOP2B-complex formation. This suggests that the mechanism of doxorubicin-mediated cardiotoxicity may involve inhibition of the normal cellular functions of TOP2B, such as transcriptional regulation, as opposed to TOP2B poisoning (Figure 6). Given that TOP2A plays a major part in the cell death of cancer cells during anthracycline-containing chemotherapy while TOP2B appears less significant (Toyoda *et al.*, 2008; Lee *et al.*, 2016), the development of TOP2A-specific drugs may provide a means to reduce TOP2B-associated cardiotoxicity caused by anthracycline therapy (Mariani *et al.*, 2015; Hasinoff *et al.*, 2016), whilst maintaining drug efficacy.

The findings presented in this article have potential clinical implications as doxorubicin, epirubicin or mitoxantrone are used in combination therapy with etoposide in a number of treatment regimes. In some regimes etoposide is given concurrently with doxorubicin, epirubicin or mitoxantrone. For example, in dose adjusted (DA) EPOCH, which is used in primary mediastinal lymphoma, doxorubicin and etoposide are actually mixed in a single bag and infused together (Wilson *et al.*, 2002). Even when the drugs are given sequentially, due to their long half-lives they could be present at the same time as etoposide (half-lives, 14.2 hours for doxorubicin, 17 hours for mitoxantrone and 33.7 hours for epirubicin) (Liston and Davis, 2017) and therefore may reduce its effectiveness. The data generated herein shows that use of etoposide in combination with anthracyclines or mitoxantrone reduces the activity of etoposide as a TOP2 poison and thus have the potential to reduce the efficacy of drug combinations.

Acknowledgements

We thank Anna Jirkovská, Thomas Nicholls, Roderick Skinner, Simon Bomken and Gareth Veal for helpful discussions.

Author contributions

Participated in research design: Atwal, Austin, Cowell

Conducted experiments: Atwal, Swan, Rowe

Performed data analysis: Atwal, Cowell, Rowe

Produced the iPSC derived cardiomyocytes Lee, Armstrong

Wrote or contributed to writing manuscript: Atwal, Austin, Cowell, Swan

References

- Atwal M, Lishman EL, Austin CA, and Cowell IG (2017) Myeloperoxidase enhances etoposide and mitoxantrone-mediated DNA damage: a target for myeloprotection in cancer chemotherapy. *Mol Pharmacol* **91**:49–57.
- Austin CA, Barot HA, Margerrison EE, Turcatti G, Wingfield P, Hayes MV, and Fisher LM (1990) Structure and partial amino acid sequence of calf thymus DNA topoisomerase II: comparison with other type II enzymes. *Biochem Biophys Res Commun* **170**:763–8.
- Binaschi M, Farinosi R, Austin CA, Fisher LM, Zunino F, and Capranico G (1998) Human DNA topoisomerase II α -dependent DNA cleavage and yeast cell killing by anthracycline analogues. *Cancer Res* **58**:1886–1892.
- Bodley A, Liu LF, Israel M, Seshadri R, Koseki Y, Giuliani FC, Kirschenbaum S, Silber R, and Potmesil M (1989) DNA Topoisomerase II-mediated Interaction of Doxorubicin and Daunorubicin Congeners with DNA. *Cancer Res* **49**:5969–5978.
- Capranico G, De Isabella P, Tinelli S, Bigioni M, and Zunino F (1993) Similar sequence specificity of mitoxantrone and VM-26 stimulation of in vitro DNA cleavage by mammalian DNA topoisomerase II. *Biochemistry* **32**:3038–3046.
- Capranico G, Kohn KW, and Pommier Y (1990) Local sequence requirements for DNA cleavage by mammalian topoisomerase II in the presence of doxorubicin. *Nucleic Acids Res* **18**:6611–6619.
- Capranico G, Zunino F, Kohn KW, and Pommier Y (1990) Sequence-selective topoisomerase II inhibition by anthracycline derivatives in SV40 DNA: relationship with DNA binding affinity and cytotoxicity. *Biochemistry* **29**:562–569.
- Chen GL, Yang L, Rowe TC, Halligan BD, Tewey KM, and Liu LF (1984) Nonintercalative antitumor drugs interfere with the breakage-reunion reaction of mammalian DNA topoisomerase II. *J Biol Chem* **259**:13560–13566.
- Classen S, Olland S, and Berger JM (2003) Structure of the topoisomerase II ATPase region and its mechanism of inhibition by the chemotherapeutic agent ICRF-187. *Proc Natl Acad Sci U S A* **100**:10629–10634.
- Coldwell KE, Cutts SM, Ognibene TJ, Henderson PT, and Phillips DR (2008) Detection of Adriamycin–DNA adducts by accelerator mass spectrometry at clinically relevant Adriamycin concentrations. *Nucleic Acids Res* **36**:e100.
- Cowell IG, and Austin CA (2012) Mechanism of generation of therapy related leukemia in response to anti-topoisomerase II agents. *Int J Environ Res Public Health* **9**:2075–2091.
- Cowell IG, Tilby MJ, and Austin CA (2011) An overview of the visualisation and quantitation of low and high MW DNA adducts using the trapped in agarose DNA immunostaining (TARDIS) assay. *Mutagenesis* **26**:253–260.

- De Angelis A, Urbanek K, Cappetta D, Piegari E, Ciuffreda LP, Rivellino A, Russo R, Esposito G, Rossi F, and Berrino L (2016) Doxorubicin cardiotoxicity and target cells: a broader perspective. *Cardio-Oncology* **2**:2.
- Dubois NC, Craft AM, Sharma P, Elliott DA, Stanley EG, Elefanty AG, Gramolini A, and Keller G (2011) SIRPA is a specific cell-surface marker for isolating cardiomyocytes derived from human pluripotent stem cells. *Nature Biotechnology* **29**:1011–1018.
- Errington F, Willmore E, Leontiou C, Tilby MJ, and Austin CA (2004) Differences in the longevity of topo II α and topo II β drug-stabilized cleavable complexes and the relationship to drug sensitivity. *Cancer Chemother Pharmacol* **53**:155–162.
- Errington F, Willmore E, Tilby MJ, Li L, Li G, Li W, Baguley BC, and Austin CA (1999) Murine transgenic cells lacking DNA topoisomerase II β are resistant to acridines and mitoxantrone: analysis of cytotoxicity and cleavable complex formation. *Mol Pharmacol* **56**:1309–1316.
- Evison BJ, Sleebs BE, Watson KG, Phillips DR, and Cutts SM (2015) Mitoxantrone, more than just another topoisomerase II poison. *Med Res Rev* **36**:248–299.
- Ferrazzi E, Woynarowski JM, Arakali A, Brenner DE, and Beerman TA (1991) DNA damage and cytotoxicity induced by metabolites of anthracycline antibiotics, doxorubicin and idarubicin. *Cancer Commun* **3**:173–180.
- Frank NE, Cusack BJ, Talley TT, Walsh GM, and Olson RD (2016) Comparative effects of doxorubicin and a doxorubicin analog, 13-deoxy, 5-iminodoxorubicin (GPX-150), on human topoisomerase II β activity and cardiac function in a chronic rabbit model. *Invest New Drugs* **34**:693–700.
- Gewirtz D (1999) A critical evaluation of the mechanisms of action proposed for the antitumor effects of the anthracycline antibiotics adriamycin and daunorubicin. *Biochem Pharmacol* **57**:727–741.
- Hasinoff BB, Wu X, Patel D, Kanagasabai R, Karmahapatra S, and Yalowich JC (2016) Mechanisms of action and reduced cardiotoxicity of pixantrone; a topoisomerase II targeting agent with cellular selectivity for the topoisomerase II α isoform. *J Pharmacol Exp Ther* **356**:397–409.
- Huelsenbeck SC, Schorr A, Roos WP, Huelsenbeck J, Henninger C, Kaina B, and Fritz G (2012) Rac1 protein signaling is required for DNA damage response stimulated by topoisomerase II poisons. *J Biol Chem* **287**:38590–38599.
- Jean SR, Tulumello DV, Riganti C, Liyanage SU, Schimmer AD, and Kelley SO (2015) Mitochondrial Targeting of Doxorubicin Eliminates Nuclear Effects Associated with Cardiotoxicity.
- Lanotte M, Martin-Thouvenin V, Najman S, Balerini P, Valensi F, and Berger R (1991) NB4, a maturation inducible cell line with t(15;17) marker isolated from a human acute promyelocytic leukemia (M3). *Blood* **77**:1080–1086.
- Lee KC, Bramley RL, Cowell IG, Jackson GH, and Austin CA (2016) Proteasomal inhibition potentiates drugs targeting DNA topoisomerase II. *Biochem Pharmacol* **103**:29–39.
- Lee MP, Sander M, and Hsieh TS (1989) Single strand DNA cleavage reaction of duplex DNA by *Drosophila* topoisomerase II. *J Biol Chem* **264**:13510–13518.

- Lian X, Zhang J, Azarin SM, Zhu K, Hazeltine LB, Bao X, Hsiao C, Kamp TJ, and Palecek SP (2013) Directed cardiomyocyte differentiation from human pluripotent stem cells by modulating Wnt/ β -catenin signaling under fully defined conditions. *Nat Protoc* **8**:162–175.
- Liston DR, and Davis M (2017) Clinically Relevant Concentrations of Anticancer Drugs: A Guide for Nonclinical Studies. *Clin Cancer Res* **23**:3489–3498.
- Long BH, Musial ST, and Brattain MG (1984) Comparison of cytotoxicity and DNA breakage activity of congeners of podophyllotoxin including VP16-213 and VM26: a quantitative structure-activity relationship. *Biochemistry* **23**:1183–1188.
- Lown JW, Hanstock CC, Bradley RD, and Scraba DG (1984) Interactions of the antitumor agents mitoxantrone and bisantrene with deoxyribonucleic acids studied by electron microscopy. *Mol Pharmacol* **25**:178–184.
- Lozzio CB, and Lozzio BB (1975) Human chronic myelogenous leukemia cell-line with positive Philadelphia chromosome. *Blood* **45**:321–334.
- Lyu YL, Kerrigan JE, Lin C-P, Azarova AM, Tsai Y-C, Ban Y, and Liu LF (2007) Topoisomerase II β mediated DNA double-strand breaks: implications in doxorubicin cardiotoxicity and prevention by dexrazoxane. *Cancer Res* **67**:8839–8846.
- Maillet A, Tan K, Chai X, Sadananda SN, Mehta A, Ooi J, Hayden MR, Pouladi MA, Ghosh S, Shim W, and Brunham LR (2016) Modeling Doxorubicin-Induced Cardiotoxicity in Human Pluripotent Stem Cell Derived-Cardiomyocytes. *Sci Rep* **6**.
- Mariani A, Bartoli A, Atwal M, Lee KC, Austin CA, and Rodriguez R (2015) Differential Targeting of Human Topoisomerase II Isoforms with Small Molecules. *J Med Chem* **58**:4851–4856.
- Minocha A, and Long BH (1984) Inhibition of the DNA catenation activity of type II topoisomerase by VP16-213 and VM26. *Biochem Biophys Res Commun* **122**:165–170.
- Minotti G, Menna P, Salvatorelli E, Cairo G, and Gianni L (2004) Anthracyclines: molecular advances and pharmacologic developments in antitumor activity and cardiotoxicity. *Pharmacol Rev* **56**:185–229.
- Montaudon D, Pourquier P, Denois F, De Tinguy-Moreaud É, Lagarde P, and Robert J (1997) Differential Stabilization of Topoisomerase-II–DNA Cleavable Complexes by Doxorubicin and Etoposide in Doxorubicin-Resistant Rat Glioblastoma Cells. *Eur J Biochem* **245**:307–315.
- Nitiss JL, Soans E, Rogojina A, Seth A, and Mishina M (2012) Topoisomerase Assays. *Curr Protoc Pharmacol* **Chapter 3**:Unit3.3.
- Patel S, Jazrawi E, Creighton AM, Austin CA, and Fisher LM (2000) Probing the interaction of the cytotoxic bisdioxopiperazine ICRF-193 with the closed enzyme clamp of human topoisomerase II α . *Mol Pharmacol* **58**:560–568.
- Pommier Y, Leo E, Zhang H, and Marchand C (2010) DNA Topoisomerases and Their Poisoning by Anticancer and Antibacterial Drugs. *Chemistry & Biology* **17**:421–433.
- Reichardt P, Tabone M-D, Mora J, Morland B, and Jones RL (2018) Risk-benefit of dexrazoxane for preventing anthracycline-related cardiotoxicity: re-evaluating the European labeling. *Future Oncology*, doi: 10.2217/fon-2018-0210.

- Roca J, Ishida R, Berger JM, Andoh T, and Wang JC (1994) Antitumor bisdioxopiperazines inhibit yeast DNA topoisomerase II by trapping the enzyme in the form of a closed protein clamp. *Proc Natl Acad Sci USA* **91**:1781–1785.
- Sinha BK, Mimnaugh EG, Rajagopalan S, and Myers CE (1989) Adriamycin activation and oxygen free radical formation in human breast tumor cells: protective role of glutathione peroxidase in adriamycin resistance. *Cancer Res* **49**:3844–3848.
- Smart DJ, Halicka HD, Schmuck G, Traganos F, Darzynkiewicz Z, and Williams GM (2008) Assessment of DNA double-strand breaks and γ H2AX induced by the topoisomerase II poisons etoposide and mitoxantrone. *Mutat Res* **641**:43–47.
- Sparano JA, Gray RJ, Makower DF, Pritchard KI, Albain KS, Hayes DF, Geyer CE, Dees EC, Goetz MP, Olson JA, Lively T, Badve SS, Saphner TJ, Wagner LI, Whelan TJ, Ellis MJ, Paik S, Wood WC, Ravdin PM, Keane MM, Gomez Moreno HL, Reddy PS, Goggins TF, Mayer IA, Brufsky AM, Toppmeyer DL, Kaklamani VG, Berenberg JL, Abrams J, and Sledge GW (2018) Adjuvant Chemotherapy Guided by a 21-Gene Expression Assay in Breast Cancer. *N Engl J Med* **379**:11–121.
- Suzuki H, Tarumoto Y, and Ohsawa M (1997) Topoisomerase II inhibitors fail to induce chromosome-type aberrations in etoposide-resistant cells: evidence for essential contribution of the cleavable complex formation to the induction of chromosome-type aberrations. *Mutagenesis* **12**:29–34.
- Swift LP, Rephaeli A, Nudelman A, Phillips DR, and Cutts SM (2006) Doxorubicin-DNA adducts induce a non-topoisomerase II-mediated form of cell death. *Cancer Res* **66**:4863–4871.
- Tewey KM, Rowe TC, Yang L, Halligan BD, and Liu LF (1984) Adriamycin-induced DNA damage mediated by mammalian DNA topoisomerase II. *Science* **226**:466–468.
- Tohyama S, Hattori F, Sano M, Hishiki T, Nagahata Y, Matsuura T, Hashimoto H, Suzuki T, Yamashita H, Satoh Y, Egashira T, Seki T, Muraoka N, Yamakawa H, Ohgino Y, Tanaka T, Yoichi M, Yuasa S, Murata M, Suematsu M, and Fukuda K (2013) Distinct metabolic flow enables large-scale purification of mouse and human pluripotent stem cell-derived cardiomyocytes. *Cell Stem Cell* **12**:127–137.
- Toyoda E, Kagaya S, Cowell IG, Kurosawa A, Kamoshita K, Nishikawa K, Iizumi S, Koyama H, Austin CA, and Adachi N (2008) NK314, a topoisomerase II inhibitor that specifically targets the alpha isoform. *J Biol Chem* **283**:23711–23720.
- Tuteja N, Phan TN, Tuteja R, Ochem A, and Falaschi A (1997) Inhibition of DNA unwinding and ATPase activities of human DNA helicase II by chemotherapeutic agents. *Biochem Biophys Res Commun* **236**:636–640.
- van Dalen EC, Caron HN, Dickinson HO, and Kremer LCM (2005) Cardioprotective interventions for cancer patients receiving anthracyclines. *Cochrane Database Syst Rev* CD003917.
- Vos SM, Tretter EM, Schmidt BH, and Berger JM (2011) All tangled up: how cells direct, manage and exploit topoisomerase function. *Nat Rev Mol Cell Biol* **12**:827–841.
- Wasserman RA, Austin CA, Fisher LM, and Wang JC (1993) Use of yeast in the study of anticancer drugs targeting DNA topoisomerases: expression of a functional recombinant human DNA topoisomerase II alpha in yeast. *Cancer Res* **53**:3591–3596.

- West KL, Meczes EL, Thorn R, Turnbull RM, Marshall R, and Austin CA (2000) Mutagenesis of E477 or K505 in the B' domain of human topoisomerase II beta increases the requirement for magnesium ions during strand passage. *Biochemistry* **39**:1223–1233.
- Willmore E, Errington F, Tilby MJ, and Austin CA (2002) Formation and longevity of idarubicin-induced DNA topoisomerase II cleavable complexes in K562 human leukaemia cells. *Biochem Pharmacol* **63**:1807–1815.
- Willmore E, Frank AJ, Padget K, Tilby MJ, and Austin CA (1998) Etoposide targets topoisomerase IIalpha and IIbeta in leukemic cells: isoform-specific cleavable complexes visualized and quantified in situ by a novel immunofluorescence technique. *Mol Pharmacol* **54**:78–85.
- Wilson WH, Grossbard ML, Pittaluga S, Cole D, Pearson D, Drbohlav N, Steinberg SM, Little RF, Janik J, Gutierrez M, Raffeld M, Staudt L, Cheson BD, Longo DL, Harris N, Jaffe ES, Chabner BA, Wittes R, and Balis F (2002) Dose-adjusted EPOCH chemotherapy for untreated large B-cell lymphomas: a pharmacodynamic approach with high efficacy. *Blood* **99**:2685–2693.
- Winterbourn CC, Gutteridge JM, and Halliwell B (1985) Doxorubicin-dependent lipid peroxidation at low partial pressures of O₂. *J Free Radic Biol Med* **1**:43–49.
- Zhang S, Liu X, Bawa-Khalfe T, Lu L-S, Lyu YL, Liu LF, and Yeh ETH (2012) Identification of the molecular basis of doxorubicin-induced cardiotoxicity. *Nat Med* **18**:1639–1642.

Footnotes

This work was supported by Breast Cancer Now (Grant 2012NovemberPhD11) and Bloodwise (Programme grant number 12031, Gordon Piller Studentship 13063).

Figure Legends

Figure 1. Dose response for formation of TOP2-DNA complexes and histone H2AX phosphorylation induced by etoposide and mitoxantrone. (A) NB4 cells were treated with the indicated concentrations of etoposide. TOP2A- and TOP2B- complexes were quantified on a cell by cell basis by the TARDIS assay, using anti-TOP2A (4566) or anti-TOP2B (4555) respectively. Data are displayed as scatterplots, each dot representing the integrated immunofluorescent signal from a single nucleus. Medians and interquartile ranges are indicated. The number of nuclei quantified for each condition are indicated above each plot. For TOP2A, fluorescent intensities were significantly above those of untreated cells for 1 μ M etoposide and above, while for TOP2B significant increase was reached by 10 μ M. **(B)** Cells treated as in (A) were analysed by immunofluorescence for phospho-S₁₃₉ histone H2AX (γ H2AX). The results are displayed as the means of the medians of replicate experiments (number of replicas indicated above each bar), normalised to 100 μ M etoposide. Error bars represent SD. **(C & D)** NB4 cells were treated with the indicated concentrations of mitoxantrone and were analysed for TOP2-DNA complexes and γ H2AX immunofluorescence as in (A) and (B) respectively. For both TOP2A and TOP2B fluorescent intensities significantly increased compared to untreated cells at all concentrations of mitoxantrone from 0.1-20 μ M. For (D) significance values were determined using one-way ANOVA with Tukey correction for multiple comparisons. Significance values shown in blue refer to comparison with untreated cells. Error bars indicate SD values.

Figure 2. Dose response for formation of TOP2-DNA complexes and histone H2AX phosphorylation induced by doxorubicin and epirubicin. (A) NB4 cells were treated with the indicated concentrations of anthracycline or etoposide. TOP2A- and TOP2B-DNA complexes were quantified as in Fig. 1. The number of cells analysed for each treatment is indicated in italics at the top of each graph. **(B)** Cells treated as in (A) and were analysed by immunofluorescence for γ H2AX. The results are displayed as the means of the medians of replicate experiments \pm SEM, normalised to 100 μ M etoposide. The number of replicates for each condition is indicated above each graph. **(C)** Proportion of cells treated with 10 μ M dox or epi that exhibit TOP2A TARDIS fluorescence above a threshold of 25% of the median value obtained with 100 μ M etoposide. Error bars indicate SD values.

Figure 3. Low anthracycline-induced TOP2-DNA complex TARDIS signal is not due to short drug incubation time or specific loss or masking of TOP2 C-terminal domain epitopes. (A) Cells were treated with 10 μ M epi for the times indicated or with etoposide (100 μ M) for 60 min and TOP2A complexes were quantified using antibody 4556 as in Fig. 1. **(B & C)** Cells were treated with the indicated TOP2 poisons for 60 minutes and TOP2 complexes were analysed using anti TOP2 antibody 4882 (raised to N-terminal 140KDa of calf thymus TOP2). Data are shown as scatterplots for one replica experiment (B) and as the means of the median values obtained from three replica experiments \pm SEM for (C). Significance values refer to comparison with untreated (control) cells by one-way ANOVA with Dunnett correction for multiple comparisons. Error bars indicated SD values.

Figure 4. Anthracyclines and mitoxantrone inhibit etoposide-induced TOP2A- and TOP2B-DNA complex stabilisation. NB4 cells **(A & B)** or K562 cells **(C & D)** were pre-incubated for one hour with doxorubicin, epirubicin, mitoxantrone or ICRF193 at the

concentration shown in the top left-hand corner of each graph. Cells were then treated with 10 μ M or 100 μ M etoposide (or vehicle control) for a further hour. TOP2A (A & C) and TOP2B (B & D) complexes were quantified as in Figure 1. The first bar in each group (grey) corresponds to treatment with etoposide alone. Data in each graph are the means of the medians from replica experiments \pm SD. The number of replicates for each condition is shown at the top of each graph. Significance tests were performed by two-way ANOVA using Dunnett's correction for multiple comparisons, (comparisons were made to etoposide treatment alone).

Figure 5. Anthracyclines and mitoxantrone inhibit etoposide-induced H2AX phosphorylation. NB4 cells were pre-treated with anthracyclines, mitoxantrone or ICRF-193 before treatment with etoposide, as in Fig. 5. Histone H2AX phosphorylation was assessed by quantitative immunofluorescence. Data in each graph are the means of the medians from replica experiments \pm SD. The number of replicates for each condition is shown at the top of each graph. Significance tests were performed as for Fig. 5.

Figure 6. TOP2 expression and induction of stable TOP2B-DNA complexes in human cardiomyocytes. (A) Induced human iPSC cardiomyocytes were stained with anti-sarcomeric actin (green) and TOP2A or TOP2B antibodies (red) and counterstained with DAPI (blue). All cells stained positive for TOP2B. Most cells were negative for TOP2A, the proportion of cells weakly (+) or strongly (++) positive for TOP2A are indicated in the Table below. (B) Cardiomyocytes were pre-treated with doxorubicin as indicated and then incubated with 100 μ M etoposide. TOP2A-DNA stabilised complexes were then quantified using the TARDIS assay as in Fig. 1. Significance values refer to comparison with control (untreated) cells (Kruskal-Wallis test with Dunn's correction for multiple comparisons)

Figure 7. Mitoxantrone, doxorubicin and epirubicin inhibit TOP2A and TOP2B mediated *in vitro* decatenation activity. Kinetoplast (kDNA) decatenation assays using recombinant TOP2A (left panels) or recombinant TOP2B (right panels) were performed in the presence of mitoxantrone (**A**), doxorubicin (**B**) or epirubicin (**C**). The gel positions of catenated and decatenated kDNA are indicated. The last lane in each gel (M) contains a marker consisting of catenated and decatenated kDNA.

Figure 8. Increasing doses of mitoxantrone, epirubicin or doxorubicin attenuate etoposide-induced *in vitro* DNA cleavage activity. Plasmid (pTCS1) cleavage assays were performed using recombinant TOP2A or TOP2B in the presence of 1mM Etoposide combined with a range of concentrations of mitoxantrone, doxorubicin or epirubicin. Gels were quantified and the degree of cleavage was normalised to that obtained with etoposide alone.

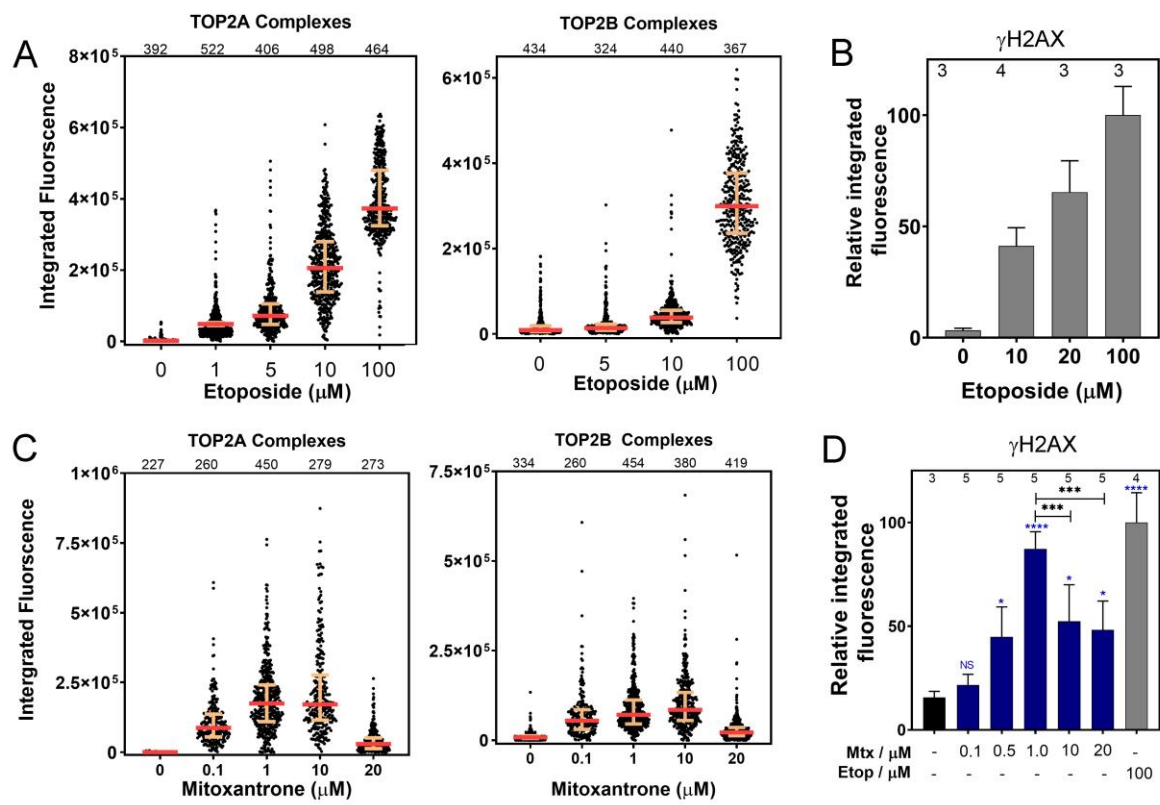


Figure 1

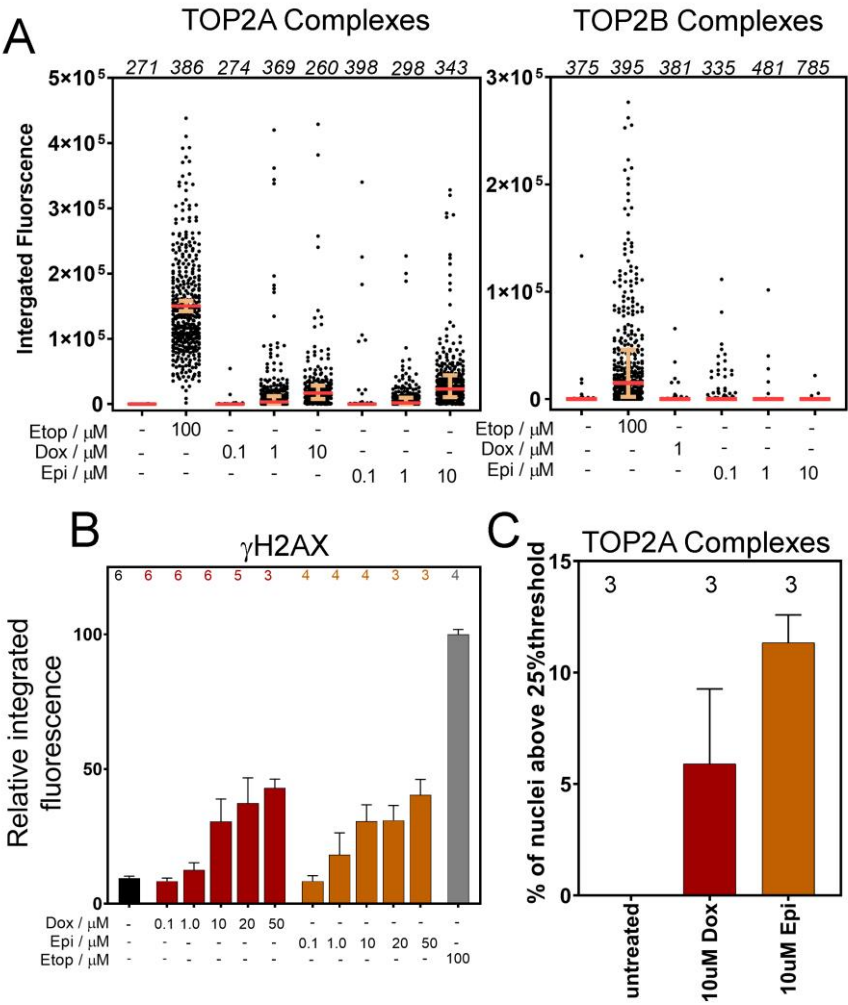


Figure 2

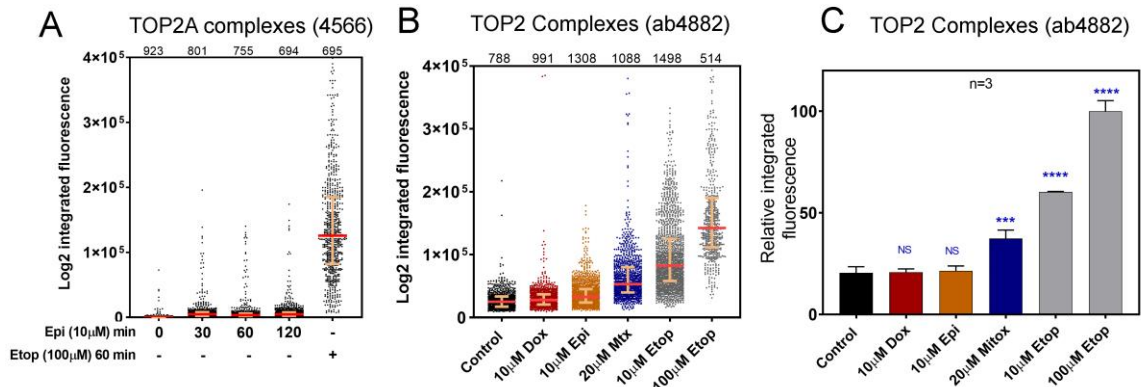


Figure 3

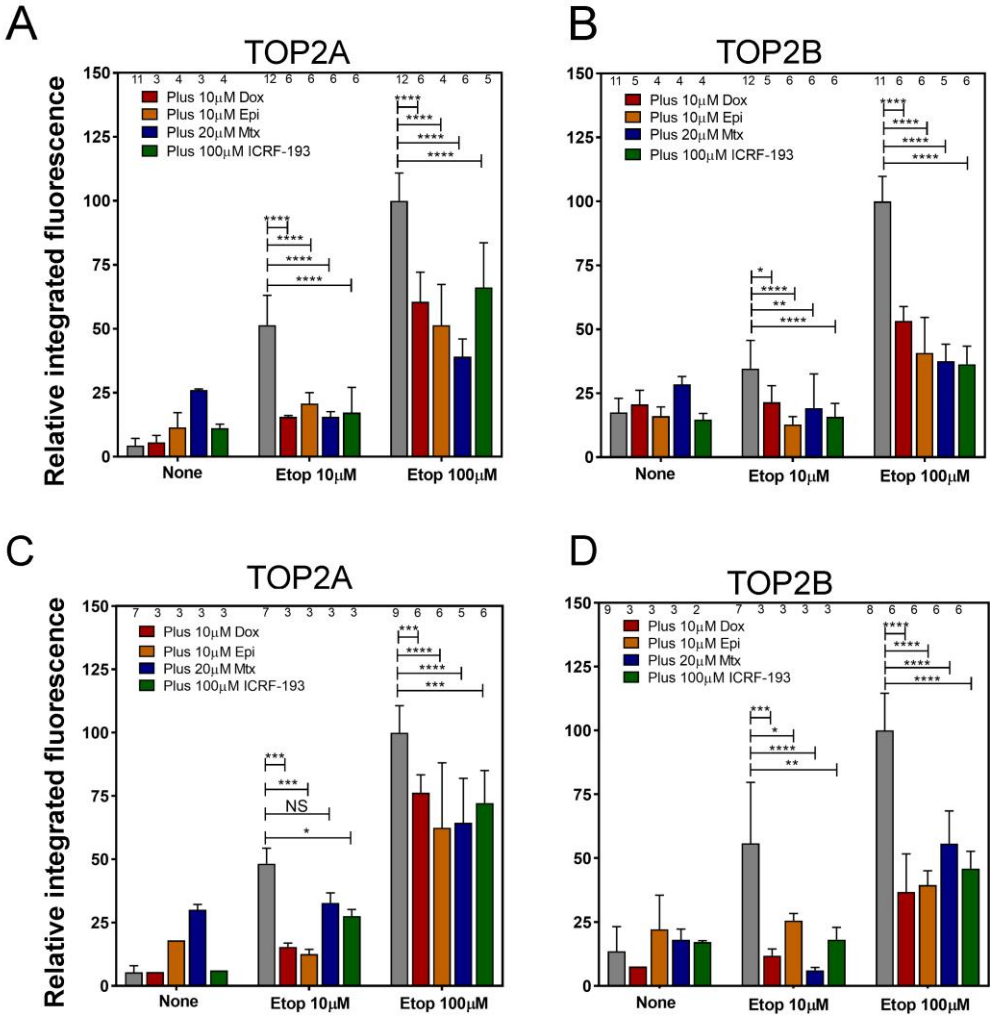


Figure 4

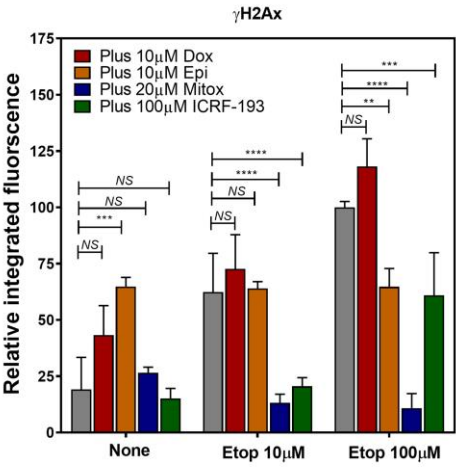


Figure 5

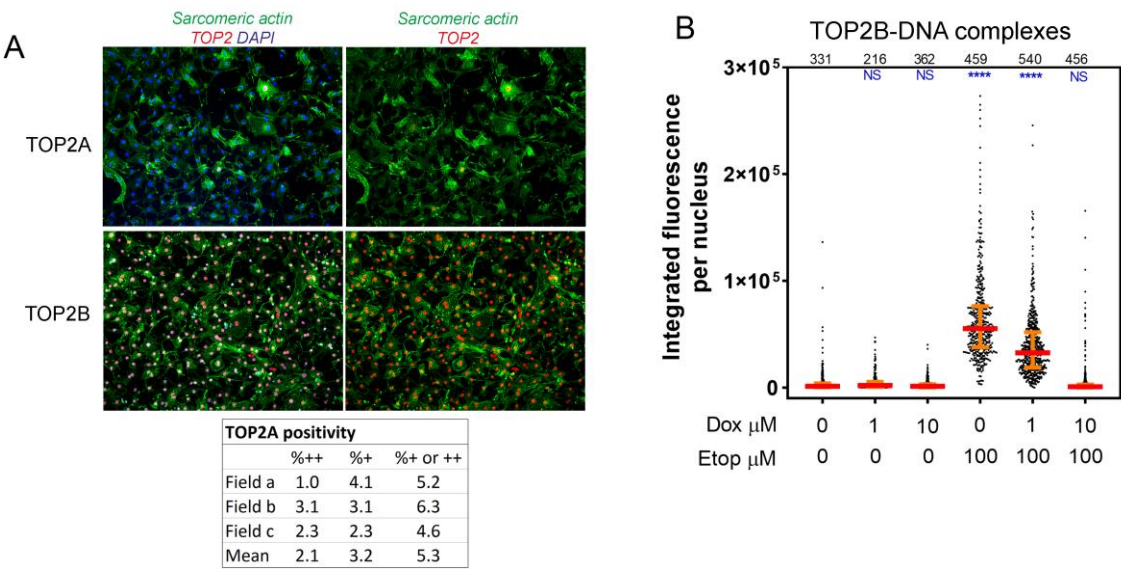


Figure 6

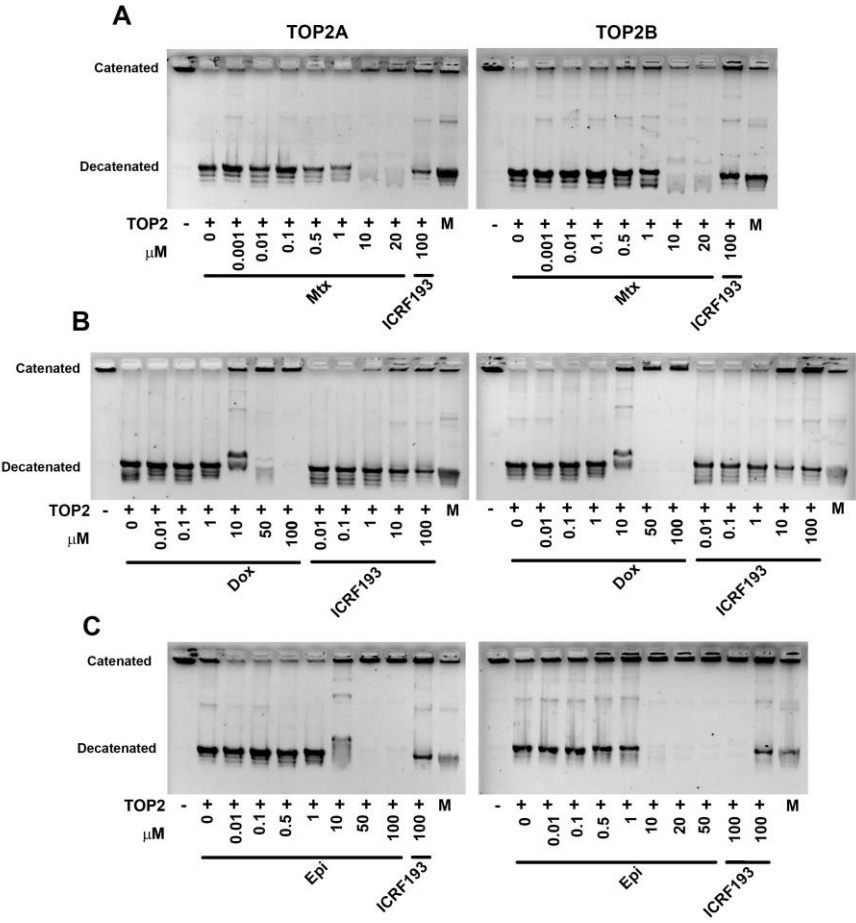


Figure 7

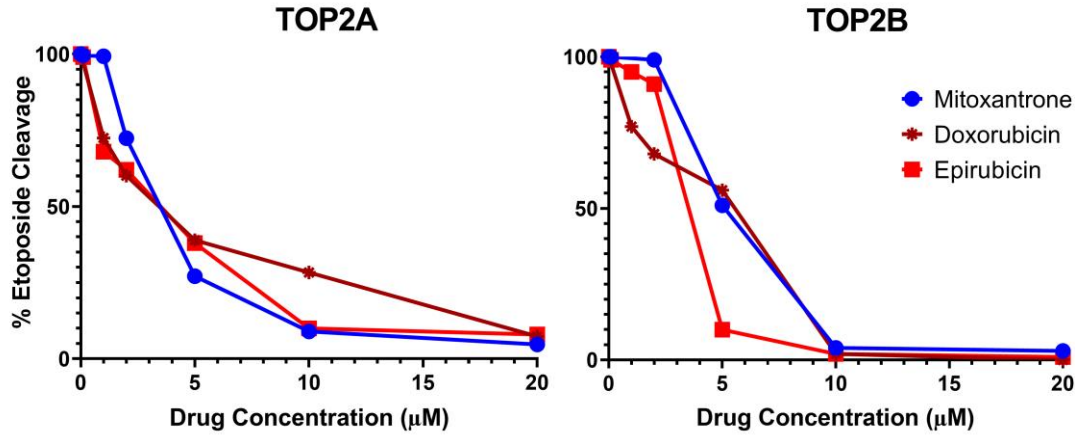


Figure 8

Supplemental Data

Intercalating TOP2 poisons attenuate topoisomerase action at higher concentrations

Mandeep Atwal, Rebecca L. Swan, Chloe Rowe, Ka C. Lee, David C Lee, Lyle Armstrong, Ian G Cowell*, Caroline A Austin*

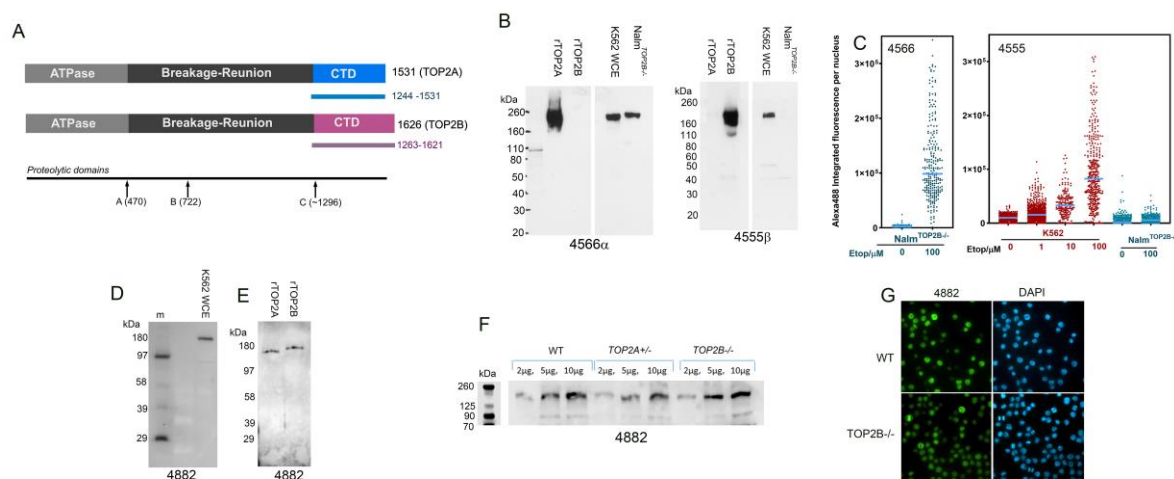
Table of Contents

Supplemental Figure Legend

Supplemental Figures 1

Supplemental Figure Legends

Supplemental Figure 1. Characteristics of inhouse antibodies used in this study. (A) TOP2 domain structure and location of immunogen polypeptide regions. The divergent C-terminal domains of TOP2A and TOP2B are coloured. Polyclonal antibodies 4566 & 4555 were raised in rabbits immunized with GST-fusion proteins containing amino acids 1244-1531 of TOP2A or 1263-1621 of TOP2B respectively. Polyclonal 4882 was produced in a rabbit immunized with a calf thymus TOP2 prep containing predominantly C-terminally truncated TOP2. **(B)** Western blot validation of antisera 4566 and 4555. rTOP2A & rTOP2B, recombinant TOP2A and B respectively, expressed in and purified from yeast; K562 WCE, whole cell extract derived from K562 cells; Nalm^{TOP2B-/-}, whole cell extract derived from TOP2B null Nalm6 cells (human pre-B leukemia cell line). **(C)** TARDIS analysis in K562 and Nalm^{TOP2B-/-} cells, confirming lack of etoposide induced signal in TOP2B null Nalm^{TOP2B-/-} cells (but efficient induction of signal in K562 cells) with antibody 4555, but efficient induction of signal in these cells with antibody 4566. **(D-F)** Western blot validation of antibody 4882 (note TOP2A and TOP2B frequently fail to resolve from each other in WCEs run on mini-gels). **(G)** Nuclear immunofluorescent staining pattern with antibody 4882 in WT and TOP2B null Nalm6 cells.



Supplemental Figure 1